

SUMO2 is essential while SUMO3 is dispensable for mouse embryonic development

Liangli Wang¹, Carolien Wansleben², Shengli Zhao³, Pei Miao¹, Wulf Paschen^{1,*} & Wei Yang^{1,**}

Abstract

Small ubiquitin-like modifier (SUMO1–3) conjugation plays a critical role in embryogenesis. Embryos deficient in the SUMO-conjugating enzyme Ubc9 die at the early postimplantation stage. *Sumo1*^{-/-} mice are viable, as SUMO2/3 can compensate for most SUMO1 functions. To uncover the role of SUMO2/3 in embryogenesis, we generated *Sumo2*- and *Sumo3*-null mutant mice. Here, we report that *Sumo3*^{-/-} mice were viable, while *Sumo2*^{-/-} embryos exhibited severe developmental delay and died at approximately embryonic day 10.5 (E10.5). We also provide evidence that SUMO2 is the predominantly expressed SUMO isoform. Furthermore, although *Sumo2*^{+/-} and *Sumo2*^{+/-};*Sumo3*^{+/-} mice lacked any overt phenotype, only 2 *Sumo2*^{+/-};*Sumo3*^{-/-} mice were found at birth in 35 litters after crossing *Sumo2*^{+/-};*Sumo3*^{+/-} with *Sumo3*^{-/-} mice, and these rare mice were considerably smaller than littermates of the other genotypes. Thus, our findings suggest that expression levels and not functional differences between SUMO2 and SUMO3 are critical for normal embryogenesis.

Keywords Embryonic development; Knockout; SUMO conjugation; SUMO2; SUMO3

Subject Categories Post-translational Modifications, Proteolysis & Proteomics; Development & Differentiation

DOI 10.15252/embr.201438534 | Received 22 January 2014 | Revised 3 April 2014 | Accepted 22 April 2014 | Published online 2 June 2014

EMBO Reports (2014) 15: 878–885

Introduction

SUMO conjugation (SUMOylation) is a protein modification that profoundly influences the stability, activity, and subcellular localization of target proteins, and modulates their interactions with DNA or partner proteins through SUMO-interacting motifs [1]. Three SUMO isoforms—SUMO1, SUMO2, and SUMO3—are ubiquitously expressed. SUMO2 and SUMO3 are almost identical in amino acid sequence and are therefore usually referred to as SUMO2/3. SUMO2/3 share about 50% identity with SUMO1. SUMOylation requires the sequential function of activating (E1), conjugating (E2),

and ligating (E3) enzymes, a process mechanistically similar to conjugation pathways of other ubiquitin-like proteins. SUMOylation is a dynamic and reversible process, as SUMO-conjugated proteins are deconjugated by sentrin/SUMO-specific proteases (SENPs).

The role of SUMO conjugation in embryonic development has been investigated in many species [2]. SUMO conjugation is indispensable for embryonic viability, as embryos deficient in the SUMO-conjugating enzyme Ubc9 die during early development [3,4]. Indeed, Ubc9-deficient mouse embryos show severe defects in chromosome segregation and die at the early postimplantation stage [3]. On the other hand, SUMO1 is not a critical determinant of embryonic development, as SUMO1-deficient mice are viable and lack any overt phenotype [5,6]. Notably, in SUMO1-deficient mice, SUMO2/3 compensates for most SUMO1 functions. For example, RanGAP1, the most prominent SUMO1-conjugated protein in wild-type embryos, is conjugated to SUMO2/3 in *Sumo1*-null mutants [5]. Whether SUMO1 can compensate for SUMO2 or SUMO3, and whether SUMO2 and SUMO3 are functionally redundant for embryonic development have yet to be determined. To better understand the SUMOylation system during embryonic development, and verify the role of SUMO2 and SUMO3 in this process, we have generated *Sumo2*- and *Sumo3*-null mutant mice.

Results and Discussion

Generation of *Sumo2*- and *Sumo3*-null mutant mice

Several studies have demonstrated that SUMO conjugation plays a critical role in embryonic development [2], but the embryonic expression patterns of SUMO isoforms have not yet been investigated. We first examined by whole-mount *in situ* hybridization the expression of *Sumo1*, *Sumo2*, and *Sumo3* in embryos using validated probes (Supplementary Fig S1). This confirmed that all 3 SUMO isoforms were ubiquitously expressed in E7.5, E8.5, and E9.5 embryos (Fig. 1A). As SUMO1 is indispensable in normal mouse development due to functional compensation by SUMO2/3 [6], the contribution of SUMO2 and SUMO3 remains intriguing in that the proteins differ by only three amino acids. In order to determine the roles of SUMO2 and SUMO3 in embryogenesis, we generated

¹ Multidisciplinary Neuroprotection Laboratories, Department of Anesthesiology, Duke University Medical Center, Durham, NC, USA

² Department of Cell Biology, Duke University Medical Center, Durham, NC, USA

³ Department of Neurobiology, Duke University Medical Center, Durham, NC, USA

*Corresponding author. Tel: +1 919 684 5576; Fax: +1 919 684 6692; E-mail: wulf.paschen@duke.edu

**Corresponding author. Tel: +1 919 684 6573; Fax: +1 919 684 6692; E-mail: wei.yang@duke.edu

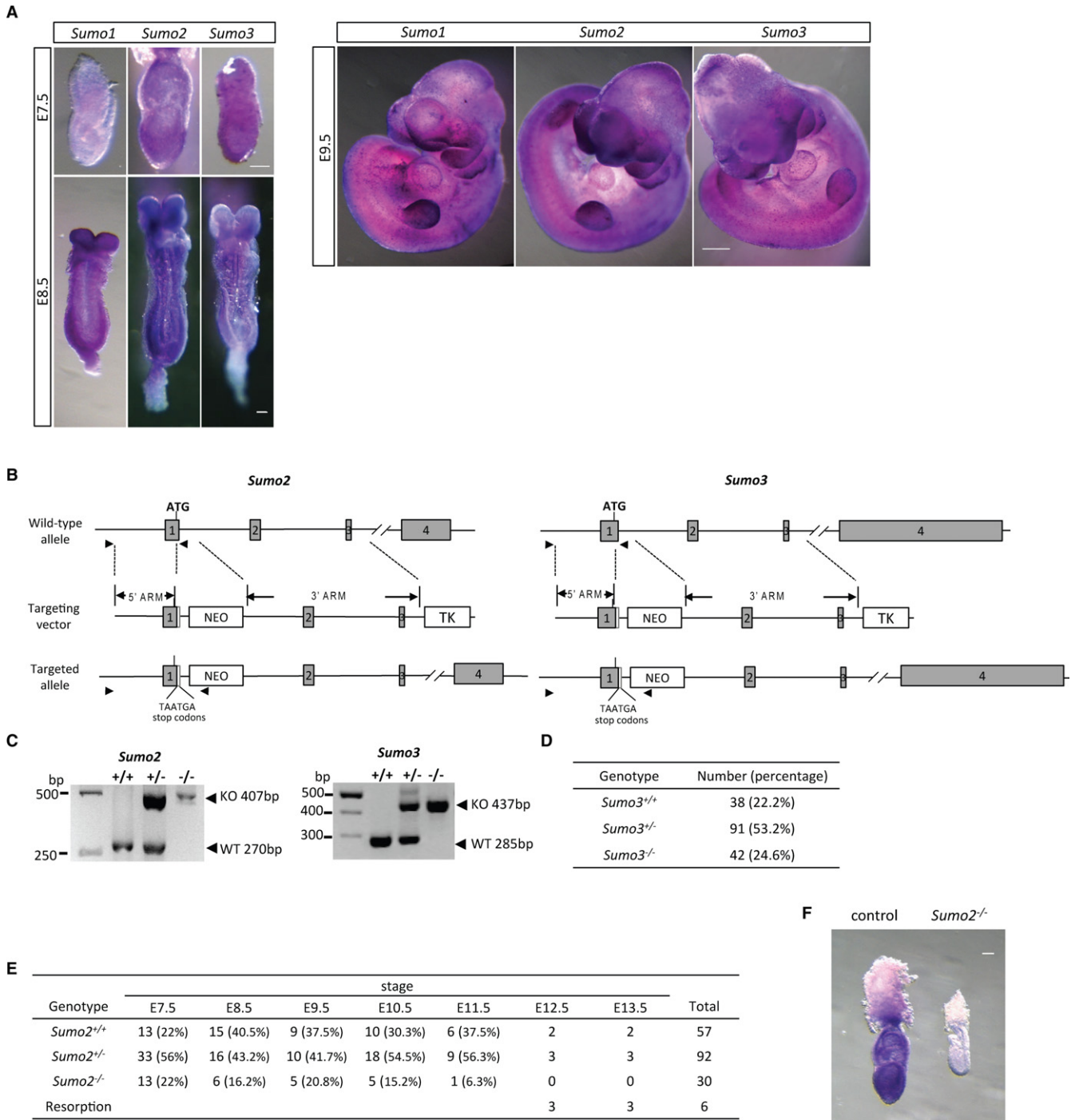


Figure 1. Targeted disruption of *Sumo2* but not *Sumo3* is lethal to embryos.

A Ubiquitous expression of *Sumo1*, *Sumo2*, and *Sumo3* in E7.5, E8.5, and E9.5 wild-type embryos. Whole-mount *in situ* hybridization analysis of *Sumo1*, *Sumo2*, and *Sumo3* expression was performed in C57BL/6 wild-type mouse embryos. The specificity of all probes was validated by comparing whole-mount *in situ* hybridization in wild-type to *Sumo1*^{-/-}, *Sumo2*^{-/-}, and *Sumo3*^{-/-} null embryos, as demonstrated in Supplementary Fig S1. Scale bars: 100 μm (left panel), 500 μm (right panel).

B Targeting strategy for *Sumo2* and *Sumo3*. The targeting vectors were designed to disrupt exon 1 by in-frame insertion of 2 stop codons and a neomycin (NEO) cassette downstream of the ATG codon. Arrowheads mark the location of primers for genotyping. Gray boxes show exons. TK, thymidine kinase cassette.

C Representative genotyping results of embryos obtained from timed *Sumo2*^{+/-} or *Sumo3*^{+/-} intercrosses. Genomic DNA prepared from extraembryonic tissue was used for PCR amplification with primers as described in (B) and Supplementary Table S1.

D Normal Mendelian distribution of newborn pups from *Sumo3*^{+/-} intercrosses.

E Summary of genotyping analysis of staged embryos from *Sumo2*^{+/-} intercrosses.

F Representative image of *Sumo2* expression by whole-mount *in situ* hybridization in a wild-type embryo (control, left) and a homozygous null embryo (*Sumo2*^{-/-}, right) at E7.5. Scale bar: 100 μm.

Sumo2- and *Sumo3*-null mutant mice. *Sumo2* and *Sumo3* genes are located on mouse chromosome 11 and 10, respectively, and have a similar genomic structure, both containing four exons (Fig. 1B). Therefore, we used the same targeting strategy to generate *Sumo2*- and *Sumo3*-null mice (Fig. 1B). In the targeted allele, 2 premature stop codons and a neomycin cassette (NEO) were placed in exon 1 to disrupt the *Sumo2* or *Sumo3* gene, thereby creating a functional null allele. The null alleles were confirmed by whole-mount *in situ* hybridization analysis of *Sumo2*^{-/-} and *Sumo3*^{-/-} embryos (Supplementary Fig S1).

Genotypes were determined by two PCRs with a 5' primer located outside the 5' homologous arm, and two 3' primers, one located immediately outside the 3' homologous arm and one within the NEO cassette (Fig. 1B,C). Both *Sumo2*^{+/-} and *Sumo3*^{+/-} mice were viable and fertile and showed no gross abnormalities in size or weight compared to the wild-type littermate controls. To generate the homozygous mutants, heterozygous mice were intercrossed. Genotypes of the progeny derived from *Sumo3*^{+/-} intercrosses showed a normal Mendelian distribution (Fig. 1D). The *Sumo3* homozygous mutants (*Sumo3*^{-/-}) were fertile and did not display

phenotypic abnormalities. However, no viable *Sumo2*^{-/-} homozygous pups from *Sumo2*^{+/-} intercrosses were found. This indicated that SUMO2 deficiency in embryos is lethal.

Sumo2^{-/-} embryos exhibited severe growth retardation and died at about E10.5

To determine the temporal profile of the lethality caused by SUMO2 deficiency, *Sumo2*^{+/-} mice were mated, and embryos were isolated and genotyped at embryonic days 7.5 to 13.5 (E7.5–E13.5). At E7.5, *Sumo2*^{-/-} embryos were detected at the expected Mendelian frequency (Fig. 1E). However, their size was smaller than that of their *Sumo2*^{+/+} littermates (Figs. 1F and 2A). At E8.5, the *Sumo2*^{-/-} embryos had developed a head fold and neural groove, and the allantoic bud was also formed. However, the allantois was found loosely attached to the chorion at E9.5 and later stages as compared to the control littermates. Furthermore, the somite structures were not visible in *Sumo2*^{-/-} embryos before E9.5, and a heart tube-like structure was not found until E10.5 (Fig. 2A), indicating severe growth retardation. A vascular system was detected in *Sumo2*^{-/-}

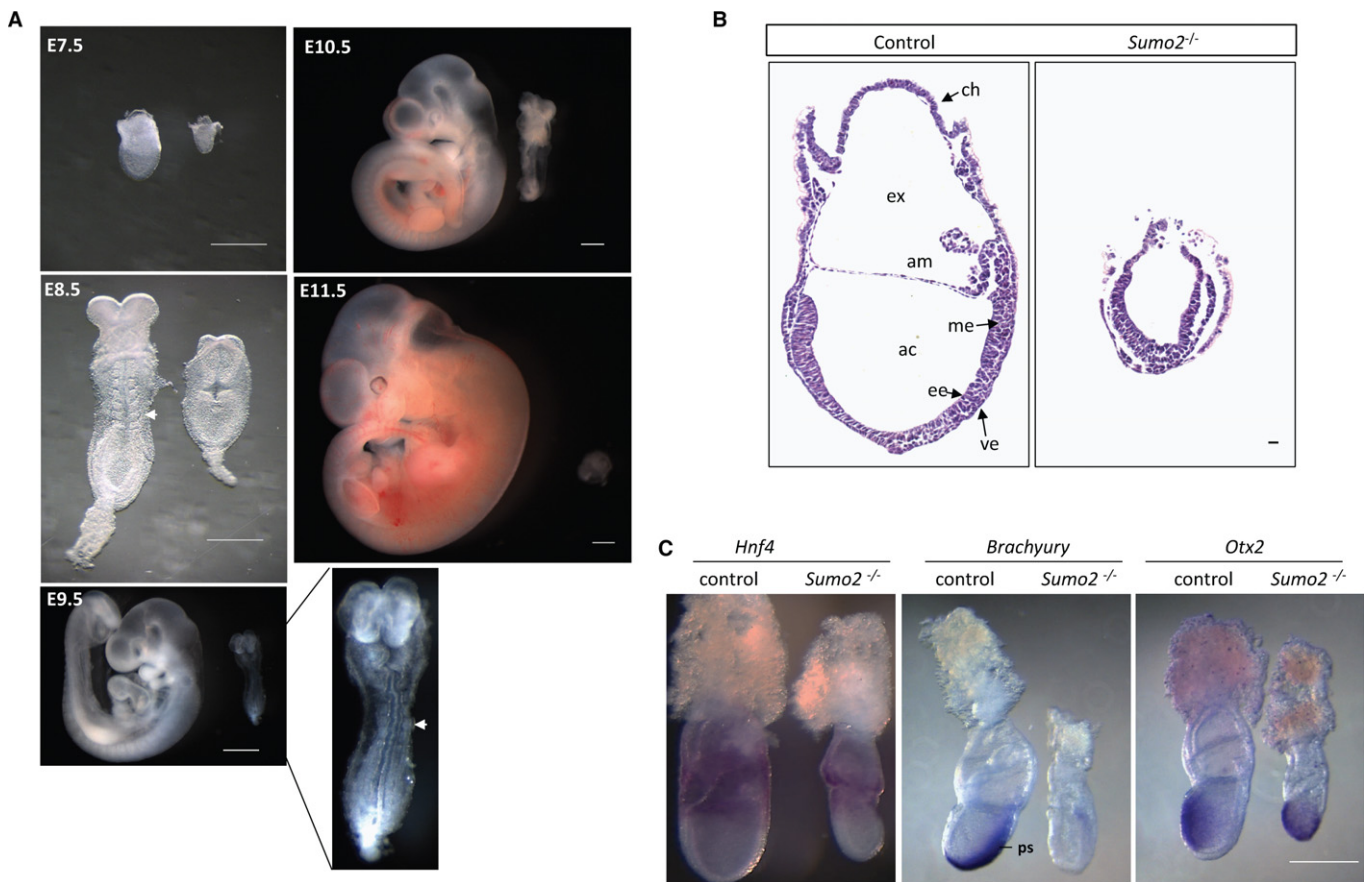


Figure 2. Developmental arrest of *Sumo2*^{-/-} embryos.

A Severe growth retardation of *Sumo2*^{-/-} embryos. Representative gross morphology of wild-type (left) and *Sumo2*^{-/-} littermate (right) embryos at different developmental stages (E7.5, E8.5, E9.5, E10.5, and E11.5). *Sumo2*^{-/-} embryo at E9.5 was enlarged to show somites (arrow). Scale bar: 500 μ m.

B Representative images of hematoxylin and eosin (H&E) staining of control and *Sumo2*^{-/-} embryos at E7.5. ee, embryonic ectoderm; me, mesoderm; ve, visceral endoderm; ch, chorion; ac, amniotic cavity; ex, exocoelomic cavity; am, amnion. Scale bar: 20 μ m.

C Representative images of whole-mount *in situ* hybridization analysis of *Hnf4* (endoderm marker), *Brachyury* (mesoderm marker), and *Otx2* (ectoderm marker) of wild-type and *Sumo2*^{-/-} littermate embryos at E7.5. ps, primitive streak.

embryos at E9.5 when somite structures were visible, using the endothelial cell-specific marker CD31 (Supplementary Fig S2). By E11.5, only resorbed debris and necrotic tissue were observed and no *Sumo2*^{-/-} embryos were recovered, suggesting that *Sumo2*-null mutants die at approximately E10.5.

Histological analysis at E7.5 showed that control embryos had a well-defined anterior–posterior axis with the proper formation of the amniotic cavity and a primitive streak, indicating that the embryo had initiated gastrulation (Fig. 2B). However, in *Sumo2*^{-/-} embryos, the amnion was not seen, although an early primitive streak with mesodermal cells was detectable between the epiblast and extraembryonic endoderm (Fig. 2B). Three germ layers (endoderm, mesoderm, and ectoderm) were confirmed in *Sumo2*^{-/-} embryos at E7.5 by whole-mount *in situ* hybridization using the germ layer-specific markers *Hnf4* (endoderm), *Brachyury* (mesoderm), and *Otx2* (ectoderm) (Fig. 2C). This suggested that gastrulation was initiated in *Sumo2*^{-/-} embryos, but the mesoderm was delayed in migrating into the extraembryonic region to form the beginning of the amnion.

To determine whether the distinct small size and growth retardation of *Sumo2*^{-/-} embryos resulted from a decrease in cellular

proliferation or an increase in cell death, we used EdU incorporation and terminal deoxynucleotidyl transferase dUTP nick end labeling (TUNEL) to analyze cell proliferation and cell death, respectively. The number of EdU-positive cells was reduced in *Sumo2*^{-/-} embryos, while the number of TUNEL-positive cells was significantly increased (Fig. 3). Therefore, both reduced cell proliferation and increased cell death likely contributed to the small size and delayed growth of *Sumo2*^{-/-} embryos.

SUMO2 is the predominant SUMO isoform

SUMO2 and SUMO3 show a high degree of similarity, as they differ by only three amino acids and cannot be distinguished by available antibodies. Therefore, it was surprising that the phenotypes of *Sumo2*- and *Sumo3*-null mutant mice were dramatically distinct. We hypothesized that expression levels of *Sumo2* and *Sumo3* differ considerably during embryogenesis and that the sum of SUMO2/3, rather than the level of individual proteins, plays the pivotal role in determining the fate of the embryo at early stages. To test this hypothesis, we used quantitative RT–PCR (qPCR) to quantify relative expression levels of *Sumo2* and *Sumo3* as well as *Sumo1* in

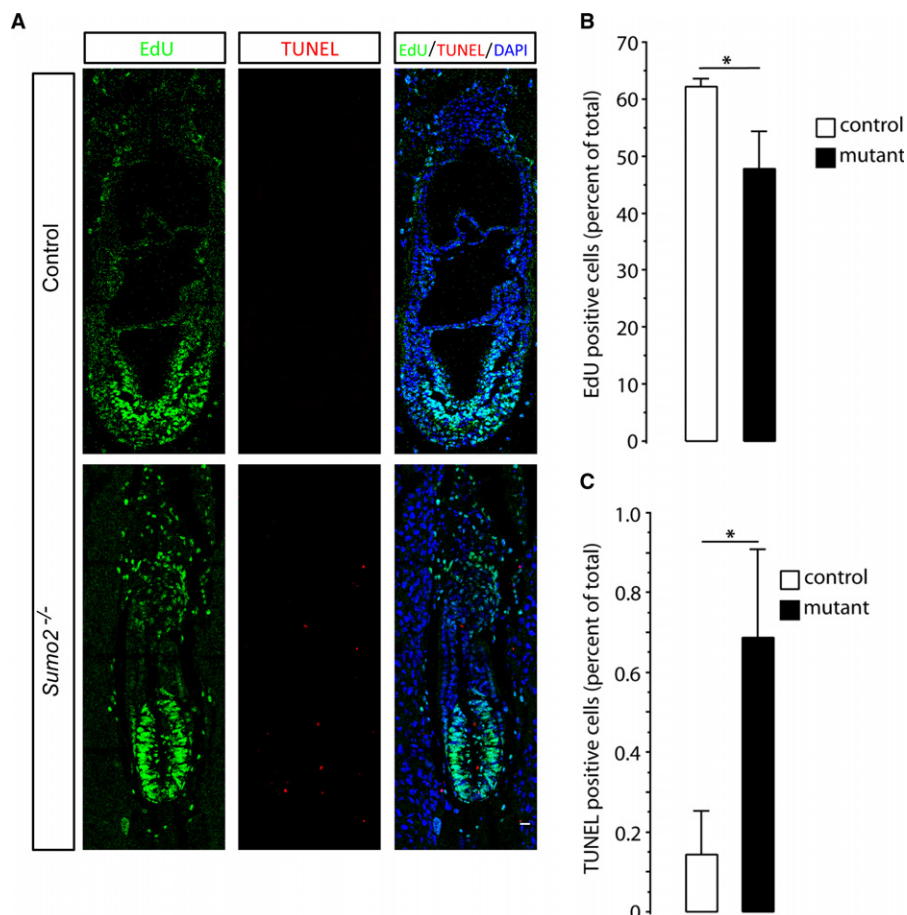


Figure 3. Compromised cell proliferation and enhanced apoptotic cell death in *Sumo2*^{-/-} embryos.

A Representative images of EdU (green) and TUNEL (red) staining of control and *Sumo2*^{-/-} embryos at E7.5. Nuclei were stained with DAPI. Scale bar: 20 μ m.
B, C Quantitative analysis of EdU and TUNEL staining. EdU-positive, TUNEL-positive, and total cells (DAPI staining) were counted, and percentages were calculated ($n = 8$ –10 sections from 3 embryos/group). Data were presented as means \pm SD. Student's *t*-test was used to calculate statistical significance; * $P < 0.05$.

wild-type C57BL/6 embryos at E7.5 and E8.5. Based on an expression level of 100% for all three *Sumo* isoforms combined, *Sumo2* accounted for about 80 and 75% at E7.5 and E8.5, respectively (Fig. 4A). In contrast, *Sumo3* accounted for only 2 and 3%, while *Sumo1* accounted for 16 and 21% at E7.5 and E8.5, respectively (Fig. 4A). Thus, SUMO2 was indeed the dominant isoform at early embryonic stages. We also evaluated expression levels of SUMO1-3 in brains, hearts, and kidneys of postnatal mice. An expression pattern similar to embryos was found at postnatal day 0 (Fig. 4A, P0). However, in adult animals, *Sumo3* levels were markedly higher and accounted for almost 20% of total *Sumos* (Fig. 4A, adult).

Next, we used Western blot to analyze the relative protein levels of SUMO2 and SUMO3 in E8.5 embryos. The SUMO2/3 antibody used in this study was generated by immunizing rabbits with purified SUMO2 protein. We confirmed that this antibody had a comparable affinity to both SUMO2 and SUMO3 (Supplementary Fig S3). Levels of SUMO2/3-conjugated proteins were markedly reduced in *Sumo2*^{-/-} compared to *Sumo2*^{+/-} and *Sumo2*^{+/+} embryos (Fig. 4B). In contrast, no significant differences in levels of SUMO2/3-conjugated proteins were found among *Sumo3*^{-/-}, *Sumo3*^{+/-}, and *Sumo3*^{+/+} embryos (Fig. 4C), thus confirming our qPCR results that SUMO2 was the predominantly expressed SUMO isoform during mouse embryogenesis. To investigate whether SUMO1 can compensate for SUMO2 or SUMO3 loss, SUMO1 Western blot analysis was performed. Notably, SUMO1 conjugation did not increase significantly in the absence of SUMO2 or SUMO3 (Fig. 4B,C), suggesting that SUMO1 cannot compensate for SUMO2 or SUMO3 loss.

Whether SUMO2 or SUMO3 is the more prominent SUMO isoform in adult mice has not been determined because available SUMO2/3 antibodies cannot distinguish between SUMO2 and SUMO3. To address this question, we collected brains, hearts, and kidneys from adult *Sumo2* or *Sumo3* mutant and wild-type mice. In contrast to embryos, there are very few SUMO2/3 conjugates in these organs in adult animals (Supplementary Fig S4). We therefore compared levels of free SUMO2/3 in those organs (*Sumo2*^{+/-} vs *Sumo2*^{+/+} and *Sumo3*^{-/-} vs *Sumo3*^{+/+}). The data revealed a more pronounced reduction of free SUMO2/3 in *Sumo2*^{+/-} mice compared with *Sumo3*^{-/-} mice (Supplementary Fig S4). Together, these results demonstrate that SUMO2 makes up the vast majority of SUMO2/3 in both embryo and adult tissues.

SUMO2/3 levels but not isoforms define embryogenesis

The most prominent findings of this study were the observations that embryos deficient in SUMO3 were viable and lacked any overt phenotype, while *Sumo2*-null mutants showed severe developmental delay and died at about E10.5. Based on earlier observations that *Ubc9*-null mutants die at the early postimplantation stage while *Sumo1*-null mutants are viable, we expected that conjugation by SUMO2/3 plays the pivotal role in embryogenesis. Therefore, the viability of *Sumo3* but not of *Sumo2*-null mutants was an unexpected finding since SUMO2 and SUMO3 are highly homologous. This raises the question of whether SUMO2 and SUMO3 are functionally different despite the high homology of more than 95%, or whether it is the total level of SUMO2/3 that drives embryogenesis. Indeed, results from this study support the latter assumption: *Sumo3* mRNA, which accounted for only about 2% of total *Sumo* mRNAs in E7.5 and E8.5 embryos (Fig. 4A), was dispensable for

embryogenesis, whereas *Sumo2*, which accounted for about 80% of total *Sumo* mRNAs, was essential.

To address the question of functional redundancy of SUMO2 and SUMO3 conjugation during embryogenesis in more detail, we first mated *Sumo2*^{+/-} with *Sumo3*^{-/-} mice. *Sumo2*^{+/-};*Sumo3*^{+/-} mice were obtained from this mating with no overt phenotype. Then, we asked whether SUMO2 is the only critical SUMO isoform required for normal embryonic development. If the specific lethal phenotype of *Sumo2*-null mutants resulted from the sole role of SUMO2 conjugation during embryonic development, we expected that reducing SUMO3 levels in heterozygous *Sumo2*^{+/-} embryos would not result in a lethal phenotype, because SUMO3 was found to be dispensable. To test this possibility, we mated *Sumo2*^{+/-};*Sumo3*^{+/-} with *Sumo3*^{-/-} mice. To our surprise, analysis of 145 progeny from a total of 35 litters revealed that 41 (28.3%) were *Sumo2*^{+/-};*Sumo3*^{+/-}, and 102 (70.2%) were *Sumo2*^{+/+};*Sumo3*^{+/-} or *Sumo2*^{+/+};*Sumo3*^{-/-}, whereas only 2 were *Sumo2*^{+/-};*Sumo3*^{-/-}, and these 2 mice were considerably smaller than littermates of other genotypes (Supplementary Fig S5). These data suggested that *Sumo2*^{+/-};*Sumo3*^{-/-} genotype is potentially lethal at late stage of embryogenesis. Indeed, *Sumo2*^{+/-};*Sumo3*^{-/-} embryos did not show a obvious phenotype at E15.5 and E17.5, but were considerably smaller at E19.5 (Supplementary Fig S5). Collectively, these findings support our hypothesis that the total levels of SUMO2/3 are critical for embryogenesis. An alternative interpretation of results would be that all 3 SUMO isoforms are dispensable and that the total level of SUMO1-3 is critical for embryogenesis. It has indeed been reported in an earlier study that SUMO isoforms are indispensable but functionally redundant in zebrafish during early development [4]. The severe defects in zebrafish embryonic development induced by SUMO1-3 deficiency could be rescued by any human or zebrafish SUMO1, SUMO2, or SUMO3 [4]. Our data can also not exclude that SUMO2 and SUMO3 have some distinct functions, and SUMO2 can compensate for SUMO3 loss only when SUMO2 levels are high. Since, however, SUMO2 and SUMO3 are highly homologous, it is unlikely that they are functionally distinct.

The results of this and earlier studies highlight the pivotal role of global SUMOylation during embryogenesis. However, embryos deficient in individual components of the SUMOylation machinery die at different embryonic stages. Embryos deficient in *Ubc9* die during an early postimplantation stage [3] when embryos deficient in SUMO1, SUMO2, or SUMO3 are still viable. *Sumo2*-null embryos failed to develop beyond the head-fold stage (E8.5), while embryos deficient in the SUMO proteases SENP1 and SENP2 die at about E12.5–E14.5 and E10, respectively [7,8]. SENP1 is specific for SUMO1-conjugated proteins *in vivo* [9], while SENP2 de-SUMOylates both SUMO1 and SUMO2/3 conjugates [10]. Taken together, these observations suggest that SUMO homeostasis must be tightly controlled during embryogenesis.

Materials and Methods

Generation of mutant mice and genotyping

This study was approved by the Duke University Animal Care and Use Committee. *Sumo1*-null mutant mice were obtained from Dr. Kuehn [5], and C57BL/6 mice were purchased from The Jackson

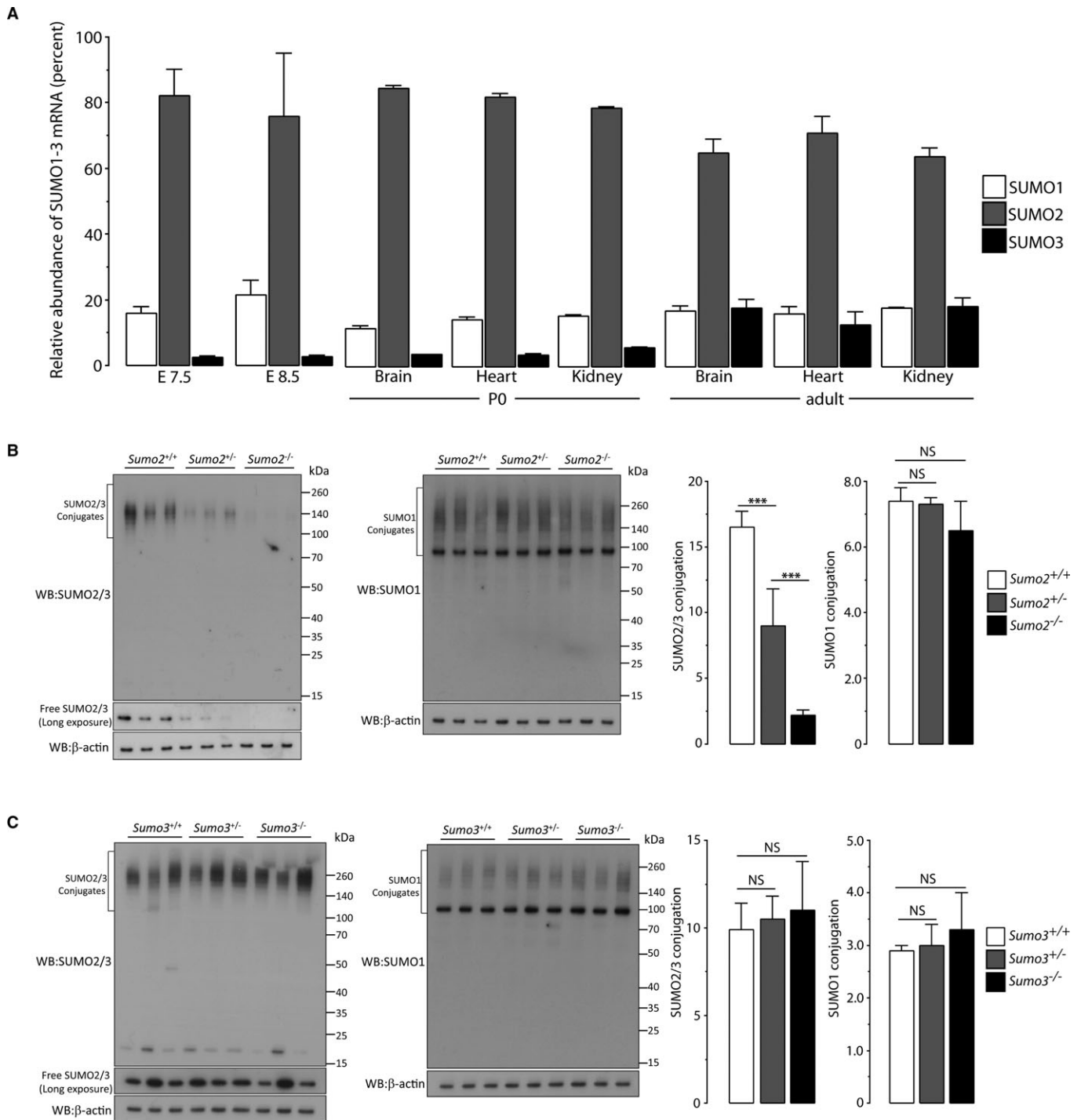


Figure 4. SUMO2 is the dominant SUMO isoform.

A Relative expression levels of *Sumo1*, *Sumo2*, and *Sumo3* in C57BL/6 wild-type embryos at E7.5 and E8.5, and in brains, hearts, and kidneys at postnatal day 0 (P0) and the adult state. Data are presented as means \pm SD ($n = 3$).

B Quantitative Western blot analysis results showed the dramatic decrease in levels of SUMO2/3-conjugated proteins in *Sumo2*^{-/-} E8.5 embryos compared to *Sumo2*^{+/-} and *Sumo2*^{+/+} E8.5 embryos ($***P < 0.001$). Notably, SUMO1 conjugation did not increase in the absence of SUMO2. The high molecular weight regions marked by brackets were used to quantify SUMO1 or SUMO2/3 conjugation. Data are presented as means \pm SD ($n = 3$). NS, not significant.

C Quantitative Western blot analysis results showed no major difference in levels of SUMO2/3- or SUMO1-conjugated proteins in *Sumo3*^{+/+}, *Sumo3*^{+/-}, and *Sumo3*^{-/-} E8.5 embryos. The high molecular weight regions marked by brackets were used to quantify SUMO1 or SUMO2/3 conjugation. Data are presented as means \pm SD ($n = 3$). NS, not significant.

Source data are available online for this figure.

Laboratory (Maine). The same strategy was used to disrupt *Sumo2* and *Sumo3* genes, as illustrated in Fig. 1B. Note that the nomenclature of SUMO2 and SUMO3 used here is in accordance with the NCBI database—protein entry number P61957 for SUMO2 and Q9Z172 for SUMO3. Two BAC clones, bMQ258k14 and bMQ457C17, containing *Sumo2* gene and *Sumo3* gene respectively, were isolated from a 129Sv mouse genomic library (Source BioScience, Nottingham, UK) and were used to retrieve the homologous arms. The targeting vectors were constructed by inserting a 5' homologous arm (*Sumo2*, 1.2 kb; *Sumo3*, 1.4 kb), 2 in-frame stop codons in exon 1 (mutated sequences are listed in Supplementary Table S1), a neomycin cassette (NEO), and a 3' homologous arm (*Sumo2*, 8 kb; *Sumo3*, 8 kb). A thymidine kinase cassette (TK) was used for negative selection. After verification by restriction analysis and partial sequencing, the targeting vectors were linearized and electroporated into mouse embryonic stem (ES) cells derived from the 129Sv strain at the Duke Neurotransgenic Laboratory. Positive ES clones were identified by PCR screening and confirmed by Southern blot analysis. Two ES clones were microinjected into blastocysts derived from C57BL/6 mice to produce chimeric mice. After the germline transmission was confirmed, heterozygous mice (*Sumo2*^{+/-} and *Sumo3*^{+/-}) were generated and crossed to produce homozygous offspring (*Sumo2*^{-/-} or *Sumo3*^{-/-}). For genotypic analysis of embryos and mice, genomic DNA was prepared from yolk sacs, whole embryos, or mouse tails. All primers for genotyping are listed in Supplementary Table S1.

Whole-mount *in situ* hybridization

Whole-mount *in situ* hybridization was conducted as described previously [11]. Briefly, antisense riboprobes were generated by *in vitro* transcription using the respective cDNA templates and were then labeled with digoxigenin (DIG)-UTP (Roche). The primers used are listed in Supplementary Table S1. Embryos were washed in PBS with 1% Tween 20 (PBT) and dehydrated by steps (25, 50, 75, and 100%) in methanol before freezing. After rehydration, embryos were treated with proteinase K (20 µg/ml) at room temperature for 15 min followed by several rinses in PBT. Embryos were then transferred to prehybridization buffer (50% formamide, 5× SSC, 2% blocking powder, 0.1% Tween 20, 0.1% CHAPS, 50 µg/ml yeast RNA, 5 mM EDTA, and 50 µg/ml heparin) at 70°C for 1 h before hybridization with probes diluted in fresh prehybridization buffer at 70°C overnight. The next day, embryos were washed 3 times with 2× SSC buffer plus 0.1% CHAPS, and 3 times with buffer (0.2× SSC and 0.1% CHAPS) at 70°C. After blocking in 10% sheep serum in KTBT buffer (50 mM Tris pH 7.5, 150 mM NaCl, 10 mM KCl, and 1% Tween 20) for 2 h at room temperature, embryos were incubated with anti-DIG antibody (1:3,000) overnight at 4°C. After intensive washes with KTBT buffer, embryos were equilibrated in NTMT buffer (100 mM NaCl, 100 mM Tris pH 9.5, 50 mM MgCl₂, and 0.1% Tween 20), and color reactions were initiated by adding the NBT/BCIP solution (1:50, Roche). Embryos were photographed on a Leica MZLFIII microscope.

Histology and immunohistochemistry analysis

Paraffin-embedded embryos were used for analysis. They were serially sectioned at 7 µm and stained with hematoxylin and eosin

(H&E) by standard procedures. To analyze for cell proliferation and apoptosis, timed pregnant heterozygous females were injected intraperitoneally with EdU (5-ethynyl-2'-deoxyuridine, 20 mg/kg, Life Technologies). Two hours later, embryos were collected and fixed in 4% paraformaldehyde. EdU staining was performed using the Click-iT EdU kit (Life Technologies). Apoptotic cells were detected by terminal deoxynucleotidyl transferase dUTP nick end labeling (TUNEL), using the *In Situ* Cell Death Detection kit (Roche, IN) according to manufacturer's instructions. Confocal images were taken using a Zeiss 710 inverted confocal microscope. The percentage of proliferating and apoptotic cells was determined by counting EdU- and TUNEL-positive cells as a percentage of the total number of cells, as determined by DAPI staining, respectively. Eight to ten sections from 3 embryos in each group (control and mutant) were used for quantification.

Quantitative RT-PCR

Total RNA was extracted from C57BL/6 embryos at E7.5 and E8.5 stages and brains, hearts, and kidneys of postnatal mice ($n = 3/\text{group}$) using TRIzol reagent (Life Technologies). Quantitative RT-PCR was performed as previously described [12]. In order to directly compare copy numbers of *Sumo1*, *Sumo2*, and *Sumo3*, an absolute quantification method based on the standard curve was used. To achieve high accuracy of quantification, a plasmid harboring the coding sequences of *Sumo1*, *Sumo2*, and *Sumo3* was constructed and used to generate all 3 standard curves from a single template. The copy number of each gene was calculated based on the corresponding standard curve. Relative levels of each gene are expressed as percentage of total levels of the three genes.

Western blotting

Embryos and mouse tissues were snap-frozen in liquid nitrogen. Proteins were extracted by sonication of frozen samples in 1× Laemmli sample buffer, followed by boiling for 10 min. Western blotting was performed as previously described [13]. Polyclonal antibody against SUMO2/3 was raised in rabbits through Custom Immunology Services provided by Covance, using purified SUMO2 proteins (BostonBiochem). Other antibodies include rabbit anti-GADPH (Cell Signaling) and mouse anti-β-actin (Sigma, MO, USA).

Statistical analysis

Data are presented as means ± SD. Statistical significance was assessed by two-tailed Student's *t*-test (EdU and TUNEL) or ANOVA followed by Fisher's PLSD test (SUMO mRNA and protein levels). The level of significance was set at $P < 0.05$.

Supplementary information for this article is available online: <http://embor.embopress.org>

Acknowledgements

The authors thank Dr. Brigid Hogan, Department of Cell Biology, Duke University Medical Center for helpful discussions and suggestions, and Kathy Gage for her excellent editorial contribution. This study was funded by NIH RO1 grants HL095552 and NS081299 to W.P. and an American Heart Association Scientist Development Grant 12SDG11950003 to W.Y.

Author contributions

LW, CW, SZ, PM, and WY performed the experiments and data analysis; WP and WY conceived the study; LW, WP, and WY wrote the manuscript.

Conflict of interest

The authors declare that they have no conflict of interest.

References

1. Geiss-Friedlander R, Melchior F (2007) Concepts in sumoylation: a decade on. *Nat Rev Mol Cell Biol* 8: 947–956
2. Lomeli H, Vazquez M (2011) Emerging roles of the SUMO pathway in development. *Cell Mol Life Sci* 68: 4045–4064
3. Nacerddine K, Lehembre F, Bhaumik M, Artus J, Cohen-Tannoudji M, Babinet C, Pandolfi PP, Dejean A (2005) The SUMO pathway is essential for nuclear integrity and chromosome segregation in mice. *Dev Cell* 9: 769–779
4. Yuan H, Zhou J, Deng M, Liu X, Le Bras M, et The H, Chen SJ, Chen Z, Liu TX, Zhu J (2010) Small ubiquitin-related modifier paralogs are indispensable but functionally redundant during early development of zebrafish. *Cell Res* 20: 185–196
5. Evdokimov E, Sharma P, Lockett SJ, Lualdi M, Kuehn MR (2008) Loss of SUMO1 in mice affects RanGAP1 localization and formation of PML nuclear bodies, but is not lethal as it can be compensated by SUMO2 or SUMO3. *J Cell Sci* 121: 4106–4113
6. Zhang FP, Mikkonen L, Toppari J, Palvimo JJ, Thesleff I, Janne OA (2008) Sumo-1 function is dispensable in normal mouse development. *Mol Cell Biol* 28: 5381–5390
7. Cheng J, Kang X, Zhang S, Yeh ET (2007) SUMO-specific protease 1 is essential for stabilization of HIF1alpha during hypoxia. *Cell* 131: 584–595
8. Kang X, Qi Y, Zuo Y, Wang Q, Zou Y, Schwartz RJ, Cheng J, Yeh ET (2010) SUMO-specific protease 2 is essential for suppression of polycomb group protein-mediated gene silencing during embryonic development. *Mol Cell* 38: 191–201
9. Sharma P, Yamada S, Lualdi M, Dasso M, Kuehn MR (2013) Senp1 is essential for desumoylating Sumo1-modified proteins but dispensable for Sumo2 and Sumo3 deconjugation in the mouse embryo. *Cell Rep* 3: 1640–1650
10. Kolli N, Mikolajczyk J, Drag M, Mukhopadhyay D, Moffatt N, Dasso M, Salvesen G, Wilkinson KD (2010) Distribution and paralogue specificity of mammalian deSUMOylating enzymes. *Biochem J* 430: 335–344
11. Wansleben C, Feitsma H, Tertoolen L, Kroon C, Guryev V, Cuppen E, Meijlink F (2010) A novel mutant allele of Ncx1: a single amino acid substitution leads to cardiac dysfunction. *Int J Dev Biol* 54: 1465–1471
12. Yang W, Sheng H, Warner DS, Paschen W (2008) Transient global cerebral ischemia induces a massive increase in protein sumoylation. *J Cereb Blood Flow Metab* 28: 269–279
13. Wang L, Ma Q, Yang W, Mackensen GB, Paschen W (2012) Moderate hypothermia induces marked increase in levels and nuclear accumulation of SUMO2/3-conjugated proteins in neurons. *J Neurochem* 123: 349–359